10.1109/ULTSYM.2009.0480

Interlaboratory Comparison of Backscatter Coefficient Estimates for Tissue-Mimicking Phantoms

Janelle J. Anderson*, Maria-Teresa Herd*, Michael R. King†, Alexander Haak†, Zachary T. Hafez†, Jun Song†, Michael L. Oelze†, Ernest L. Madsen*, James A. Zagzebski*, William D. O'Brien, Jr.†, and Timothy J. Hall*
*Medical Physics Department, University of Wisconsin (UW), Madison, Wisconsin 53705
†Bioacoustics Research Laboratory (BRL), University of Illinois, Urbana-Champaign, Illinois 61820

***Abstract*—Backscatter in ultrasound is a useful property for characterizing tissues and several groups have reported methods for estimating this property. However, previous inter-laboratory comparisons of backscatter coefficient (BSC) estimates have shown variability in BSC results, were only acquired over a relatively narrow frequency range, and lacked reference to any independent predictions from scattering theory. With highly variable results and no claim of a "right" answer, our goal was to compare Faran scattering theory predictions with cooperatively measured backscatter coefficients for low- and tissue-like attenuating phantoms containing glass spheres scatterers of different sizes for frequencies from 1 to 12 MHz. Backscatter coefficients were measured using two different planar reflector techniques at two laboratories for two groups of phantoms. The use of spherical glass scatterers with well-characterized size distributions allowed calculation of the expected backscatter coefficients using Faran's theory. Results showed excellent agreement between both labs' BSC measurements and with Faran's theory. Excellent agreement with the predictions of Faran's theory demonstrates the ability to accurately estimate both effective scatterer size and acoustic concentrations, all of which may prove useful parameters for clinical diagnostic applications in tissue characterization. (Supported by NIH/NCI R01CA111289.)**

I. Introduction

The backscatter coefficient (BSC) in ultrasound is a useful property for characterizing tissues. It is defined as the differential scattering cross section per unit volume for a scattering angle of 180 degrees [1]. Like most ultrasonic tissue characterization parameters, BSC is most useful if it is accurate. A commonly used reference for comparison of BSC measurement accuracy is Faran's scattering theory [2]. Faran's work predicts scattering from a small, single rigid spherical or cylindrical scatterer, assuming the scatterer is within a non-viscous medium. Many studies have tested Faran's theory against experimentally determined BSC estimates using test phantoms. For example, Burke et al. showed that despite Faran's non-viscous medium assumption, phantoms with a viscous agar background could be measured and produce angle-dependent scattering estimates in good agreement with Faran [3]. Additionally, phantoms containing a single spherical scatterer of different sizes and of different materials (such as graphite and glass) could also be measured and found to produce results consistent with Faran's predictions. Expanding from single spherical scatterers, Faran-predicted scattering theory was also demonstrated in measurements of phantoms containing multiple small spherical scatterers [4]. Additional phantom studies revealed that BSC could be accurately determined independently of transducer-to-scattering-volume distance, opening up the possibility for an instrument-independent method for determining BSC [5]–[7]. Further phantom-based studies demonstrated the ability to obtain BSC estimates and even BSC images up to 12MHz using a variety of array transducers on clinical scanners [8], [9]. In order to determine the diagnostic capabilities of BSC and further improve BSC estimation, it is vital that measurement accuracy be demonstrated among research groups active in this area, despite differences in methodologies. To do this, several inter-laboratory studies were completed to compare measurement accuracy of ultrasonic backscatter, attenuation, and sound speed measurements of several phantoms. The first comparison showed that attenuation measurements among groups agreed, but variable results existed for sound speed and backscatter measurements [10]. A later comparison demonstrated that BSC estimation was still highly variable in absolute magnitude, but the frequency-dependence tended to agree well [11]. These interlaboratory comparisons were limited in several ways. First, groups participating in these studies only obtained measurements over a relatively narrow frequency range of 1 to 9MHz. Second, no comparison with the scattering theory was done to examine BSC estimate accuracy. Third, BSC estimate comparison was made for phantoms with relatively low ka (product of the wave number and scatterer radius; largest was $ka \simeq 1.6$).

The goal of this study was to compare BSC accuracy using well-characterized phantoms of both tissue-like attenuating and low-attenuating materials with moderately low to high ka's (about .01 to 4). The phantoms contained spherical glass bead scatterers with known size distributions allowing accurate predictions of BSC using Faran's theory. All of the phantoms were measured over the frequency range of 1 to 12MHz at two different laboratories: the Ultrasound Research Group at University of Wisconsin-Madison (UW) and the Bioacoustics Research Lab at University of Illinois Urbana-Champaign (BRL).

II. METHODS

A. Materials

Two different groups of phantoms were created: phantoms with low attenuation (LA) and phantoms with tissue-like attenuation (TLA). Two LA phantoms were used: the 41 μm glass beads in agar phantom, which had a very narrow distribution of scatterer sizes (41$\pm$2 μm) and low ka at these frequencies; and the 150-180 μm glass beads in agar phantom, which had a slightly broader distribution of scatterer sizes (160$\pm$60 μm) and higher ka. Seven tissue-like attenuation phantoms (TLA) were created, all of which had relatively low ka but the glass type, diameter distribution and number density of scatterers within each phantom differed (see Tables I and II) as did the attenuation coefficient.

Glass Type	Borosilicate	Soda Lime
Sound Speed	6050 m/s	5572 m/s
Mass Density	2.2 g/cm^3	2.38 g/cm^3
Bead Source	Potters 3000E	Potters 2900A Potters 2024A Duke 41 μm

TABLE I: Characteristics of the spherical scatterers used in the phantoms.

The phantoms were all shaped like hockey pucks and were constructed as described by Madsen et al. [12]. The background material for the TLA phantoms was a mixture of gelatin and ultra-filtered milk, whereas the LA phantoms had a weakly scattering 2% agar background. Glass bead scatterers were used in all of the phantoms and are described in Table I (Potters Industries, Inc., Valley Forge, PA; Thermo Fisher Scientific (formerly Duke Scientific), Inc., Waltham, MA). The distributions of scatterer sizes for each sphere type were measured manually using optical microscopy [4] and are presented as histograms in figure 1.

B. UW Experimental Procedures

Sound speed and attenuation coefficients were measured using a through-transmission technique [12] at 22 °C and five discrete frequencies between 2.25 and 10MHz. A Wavetek model 81 function generator was used to excite the transducer, and a LeCroy model LT342 oscilloscope was used to manually record time-shifts and amplitude changes with and without the phantom between the transmitter and receiver path. Quadratic curve fitting was done to determine the attenuation coefficient in dB cm-1 MHz-1.

To measure the backscatter coefficient, a water tank, LeCroy model LT342 oscilloscope, Panametrics model 5800 pulser/receiver, Aerotech Unidex 11 stepper motor control unit, and four spherically focused transducers (3.5MHz with 95 mm focus, 5MHz with 54 mm focus, 7.5MHz with 94 mm focus, and 10MHz with 51 mm focus) were used.

Each phantom's surface was aligned at the transducer focus using vertical and horizontal scans. Once aligned a gate length of 10μs after a delay of 4μs was applied. The 4μs delay avoided specular reflections from the phantom surface. The phantom was raster scanned in one plane using a 40mm by 40mm area at 4mm steps for a total of 121 data steps, each step averaged 100 scans (to reduce electronic noise). Echo signals were also acquired from a quartz planar reflector with exactly the same setup used for acquiring echo data from the phantoms. The planar reflector face was placed at the focus for the transducer and aligned by maximizing the received signal amplitude across the planar reflector. The received data signal was averaged over 100 scans.

Data was analyzed employing the method described by Madsen et al. [1] A Hamming window was applied to the data and the power spectrum estimated for the 121 waveforms. This was divided by the reference spectrum from the quartz planar reflector to account for equipment properties.

C. BRL Experimental Procedures

Sound speed and attenuation were measured using the standard through-transmission technique [12]. For BSC estimation, the phantom was ultrasonically scanned using three single-element transducers with center frequencies of 3.5 MHz, 7.5 MHz, and 13 MHz. The scans were conducted in a tank filled with degassed water. Panametrics model 5900 pulser/receiver was used to excite the transducer. An A/D converter (Signatec PDA14-200 A/D converter) combined with a customized LabView oscilloscope program were used to record the waveforms. A Daedal motion system (Parker-Hannifin Corporation) was used for scanning.

The scanning procedure for each transducer and phantom began by performing a planar reference scan. Echo signals from a water-Plexiglas interface were recorded over the axial range for which the reflection is greater than half the reflected magnitude at the focus; within this range, the reflected signal was recorded at half-wavelength intervals. Next, the transducer focus was positioned below the surface of the phantom at a distance of half the length of the ROI to be used for processing plus 1 mm. A raster scan was then performed, with A-lines recorded at intervals equal to half of the beam width. Generally, the scan covered a sufficient length so that several ROIs could be extracted and processed from each scan.

The backscatter coefficients were computed from the raw scan data using the method of Insana and Hall [13]. This method accounts for equipment dependent effects by dividing the power spectral magnitude of the echo signals from the phantom by those of the reference (Plexiglas) signals. A correction was made for the layer of Saran covering the phantom [10]. Also, attenuation was compensated for by assuming that the attenuation had a linear dependence on frequency and using values of 0.08 dB/cm-MHz at 3.5 MHz, 0.112 dB/cm-MHz at 7.5 MHz, and 0.191 dB/cm-MHz at 13 MHz.

III. RESULTS

In each plot of the BSC data, the Faran-predicted BSC is displayed as a smooth solid black curve. The other curves represent measured BSC by UW (red lines) and BRL (blue lines). Different line styles correspond to specific transducers used for data acquisition.

	F1	F2	M1 & M2	M3	A1	A2
Sphere Concentration	2 g/L	8 g/L	4 g/L	4 g/L	2 g/L	8 g/L
Sphere Type	3000E	3000E	3000E	3000E	2900A	2900A
Sphere Size (μm)	5–40	5–40	5–40	5–40	45–53	45–53
Background Material	3:1 Gel to Milk	3:1 Gel to Milk	3:1 Gel to Milk	3:1 Gel to Milk	3:1 Gel to Milk	3:1 Gel to Milk
Background Density (g/cm^3)	1.04	1.04	1.04	1.04	1.04	1.04
Sound Speed (m/s)	1552	1553	1549 1552	1559	1548	1549
Attenuation (dB/(cm-MHz))	0.5	0.5	.0.45	0.7	0.45	0.48

TABLE II: Tissue-like attenuation (TLA) phantoms and their compositions. Note the difference between the F phantoms is their sphere number densities; the difference between the M phantoms is their attenuation values; and the difference between the A phantoms is their sphere number densities. The differences between the F and A phantoms are the glass sphere type and sizes used. Important physical properties for each glass type can be found in Table I.

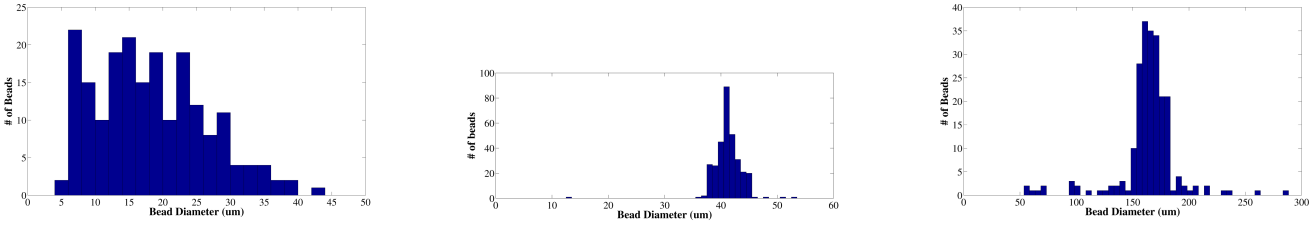

(a) Potter's 3000E (b) Duke Scientific 41μm. (c) Potter's 2900 sieved from 150-180μm

Fig. 1: Diameter distributions for the glass bead scatterers.

A. TLA Phantoms

For the F1 and F2 phantoms, both groups' measurements agree quite well with each other and with the Faran-predicted scattering (Figure 2). Additionally, the elevated backscatter from different number densities among these phantoms is clearly distinguishable.

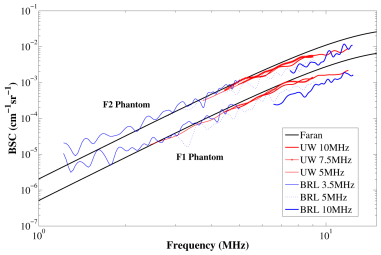

Fig. 2: BSC for the F1 and F2 TLA phantoms.

The M1, M2, and M3 phantoms all had the same Faran-predicted BSC (Figures 3a, 3b, 3c). Both groups' measurements show good agreement with the theory over the measured frequency range.

For the A1 and A2 phantoms, both groups' measurements again agree well with each other and with Faran (Figure 4). Here again, the difference in number densities between the two phantoms is visualized by the different BSC measurements and Faran predictions for each phantom.

B. LA Phantoms

The BSC measurements for the 41 μm Glass Spheres in Agar phantom are shown in figure 5a. Both the BRL and the UW results agree very closely with Faran. For the 150-180 μm Glass Spheres in Agar phantom, the UW results agree

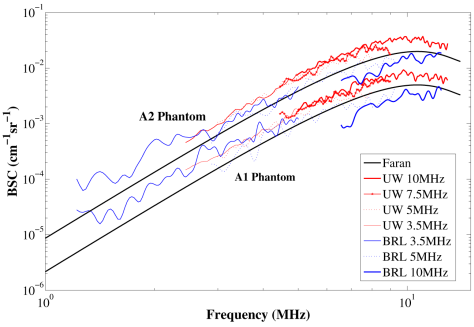

Fig. 4: BSC measurements for the A1 and A2 TLA phantoms compared to Faran.

well with Faran, but the BRL results are biased low (Figure 5b). Despite this magnitude difference, both groups' frequency dependence agrees with Faran predictions.

IV. Conclusions

With the exception of the 150-180 μm glass spheres in agar phantom, the BSC estimation methods used at BRL and UW both produced measurements over the range of 1 to 12 MHz that agreed with Faran's scattering theory both in frequency dependence and scattering magnitude. The phantoms used in this study were constructed so their Faran predicted scattering could be easily determined. Additionally, broader distributions of scatterer sizes and higher ka's were used in these phantoms than were used in previous inter-laboratory comparisons.

The magnitude difference between the BRL and UW results for the 150-180 μm Glass Spheres in Agar phantom is yet to

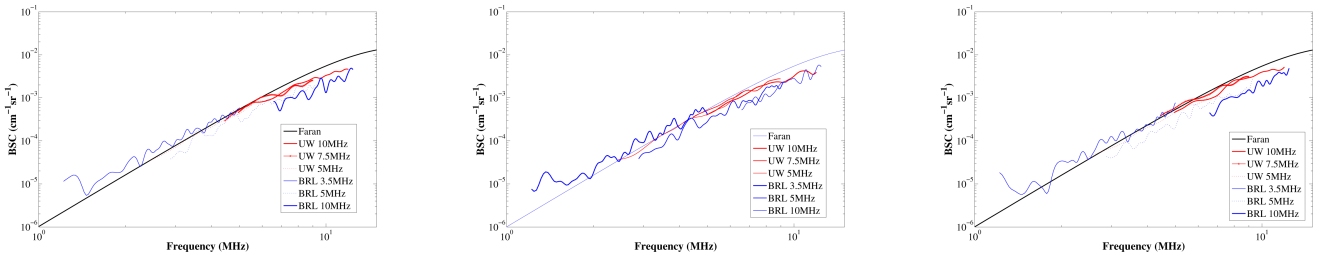

(a) M1 phantom (b) M2 phantom (c) M3 phantom

Fig. 3: Measured and predicted BSC for the "M" series phantoms.

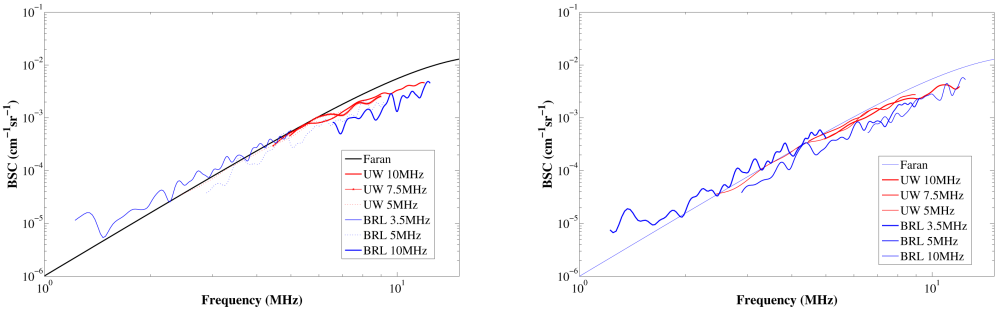

(a) 41 μm glass spheres (b) 150-180 μm glass spheres

Fig. 5: BSC measurements for the LA phantom compared to Faran.

be resolved.

The accuracy of these BSC measurements will allow us to obtain more accurate BSC-derived parameters, such as effective scatterer size and acoustic concentration, and to use these parameters to improve characterization of tissues. Furthermore, accurate BSC estimates for various tissues will help establish a means to quantify echogenicity on an absolute scale rather than relative scales. The next direction for this work is to extend into higher frequencies of analysis, continue validating BSC estimation accuracy using different methods on well-characterized phantoms, and continue comparing with scattering theory.

V. Acknowledgements

This work supported by NIH/NCI R01CA111289.

References

[1] E. L. Madsen, M. F. Insana, and J. A. Zagzebski, "Method of data reduction for accurate determination of acoustic backscatter coefficients," *J Acoust Soc Am*, vol. 76, no. 3, pp. 913–923, 1984.

[2] J. J. Faran, "Sound scattering by solid cylinders and spheres," *J Acoust Soc Am*, vol. 23, no. 4, pp. 405–418, 1951.

[3] T. M. Burke, M. M. Goodsitt, E. L. Madsen, and J. A. Zagzebski, "Angular distribution of scattered ultrasound from a single steel sphere in agar gelatin: A comparison between theory and experiment," *Ultrasonic Imaging*, vol. 6, pp. 342–347, 1984.

[4] W. J. Davros, J. A. Zagzebski, and E. L. Madsen, "Frequency-dependent angular scattering of ultrasound by tissue-mimicking materials and excised tissue," *J Acoust Soc Am*, vol. 80, no. 1, pp. 229–237, 1986.

[5] M. F. Insana, E. L. Madsen, T. J. Hall, and J. A. Zagzebski, "Tests of the accuracy of a data reduction method for determination of acoustic backscatter coefficients," *J Acoust Soc Am*, vol. 79, no. 5, pp. 1230–1236, 1986.

[6] T. J. Hall, E. L. Madsen, J. A. Zagzebski, and E. J. Boote, "Accurate depth-independent determination of acoustic backscatter coefficients with focused transducers," *Journal of Acoustical Society of America*, vol. 85, p. 2410, 1989.

[7] E. J. Boote, J. A. Zagzebski, E. L. Madsen, and T. J. Hall, "Instrument-independent acoustic backscatter coefficient imaging," *Ultrasonic Imaging*, vol. 10, no. 2, pp. 121–138, 1988.

[8] E. J. Boote, J. A. Zagzebski, and E. L. Madsen, "Backscatter coefficient imaging using a clinical scanner," *Medical Physics*, vol. 19, p. 1145, 1992.

[9] M. F. Insana, T. J. Hall, and L. T. Cook, "Backscatter coefficient estimation using array transducers," *IEEE Trans Ultrason, Ferroelec, Freq Cont*, vol. 41, no. 5, pp. 714–723, 1994.

[10] E. L. Madsen, F. Dong, G. R. Frank, B. S. Garra, K. A. Wear, T. A. Wilson, J. A. Zagzebski, H. L. Miller, K. K. Shung, S. H. Wang, E. J. Feleppa, T. Liu, W. D. O'Brien, K. A. Topp, N. T. Sanghvi, A. V. Zaitsev, T. J. Hall, J. B. Fowlkes, O. D. Kripfgans, and J. G. Miller, "Interlaboratory comparison of ultrasonic backscatter, attenuation and speed measurements," *J Ultrasound Med*, vol. 18, pp. 615–31, 1999.

[11] K. A. Wear, T. A. Stiles, G. R. Frank, E. L. Madsen, F. Cheng, E. J. Feleppa, C. S. Hall, B. Kim, P. Lee, W. D. O'Brien, M. L. Oelze, B. Raju, K. K. Shung, T. A. Wilson, and J. Yuan, "Interlaboratory comparison of ultrasonic backscatter coefficient measurements from 2 to 9 mhz," *Journal of Ultrasound in Medicine*, vol. 24, p. 1235, 2005.

[12] E. L. Madsen, J. A. Zagzebski, R. A. Banjavic, and R. E. Jutila, "Tissue mimicking materials for ultrasound phantoms," *Med Phys*, vol. 5, pp. 391–394, 1978.

[13] M. F. Insana and T. J. Hall, "Parametric ultrasound imaging from backscatter coefficient measurements: image formation and interpretation," *Ultrasonic Imaging*, vol. 12, pp. 245–267, 1990.